X-ray imaging of relativistic shock in hotspots of Pictor A radio galaxy

Rameshan Thimmappa[1], **Ł. Stawarz,**[1] **V. Marchenko**[1], **K. Balasubramaniam**[1], **U.Pajdosz**[1],

[1]Astronomical Observatory, Jagiellonian University, 30-244 Krakow, Poland
email : rameshan@oa.uj.edu.pl

Abstract

Here we present some preliminary results of our analysis of the *Chandra* observations of the Western and Eastern hotspots in the Pictor A radio galaxy. All the available *Chandra* data for the target, consisting of multiple pointings spanning over 15 years and amounting to the total exposure time of 464ks, have been included in the analysis. In particular, with the image deconvolution method we studied the X-ray morphology and variability in the Western hotspot region, confirming the flux changes taking place in the source on the timescale of years, and clearly resolving the bow-shock structure of the hotspot. For the Eastern hotspot, we performed a detailed spectral analysis of various regions selected based on the observed correlation between the X-ray intensity and the polarised radio intensity. All in all, our findings suggests a substantial substructure of the targeted relativistic shocks, and this has profound consequences for understanding acceleration of high-energy particles at relativistic shocks, as well as the pressure balance between magnetic field and ultra-relativistic electrons within the extended lobes of radio galaxies.

Introduction

Pictor A is one of the most prominent radio galaxies in the Southern sky. We have performed a novel analysis of the diffuse X-ray emission from and around the terminal shocks (below: "hotspots") in the system, formed when relativistic jets that originate within the active nucleus interact with the intergalactic medium (IGM), at hundreds-of-kpc distances from the host galaxy. Pictor A is in general an excellent candidate for a comprehensive study of the physics of relativistic jets, due to its large angular size and high surface brightness (in both radio and X-ray domains) of the extended lobes. In our detailed analysis, we therefore hope to constrain the spatial and energy distribution of ultra-relativistic electrons, as well as the magnetic field structure in the source.

The Data

Chandra has observed Pictor A on 14 separate occasions over the past 15 years, for a total of 464 ks of the observing time, as listed below in the table.

ObsID	Date	exp-time (ks)	θ_{HS}
346	2000-01-18	25.8	3.46
3090	2002-09-17	46.4	0.09
4369	2002-09-22	49.1	0.09
12039	2009-12-07	23.7	3.35
12040	2009-12-09	17.3	3.35
11586	2009-12-12	14.3	3.35
14357	2012-06-17	49.3	3.06
14221	2012-11-06	37.5	3.10
15580	2012-11-08	10.5	3.10
14222	2014-01-17	45.4	3.30
16478	2015-01-09	26.8	3.30
17574	2015-01-10	18.6	3.32

All the data were reprocessed in the standard aspect using CIAO 4.10 (using the `chandra_repro` script) and Calibration database CALDB 4.7.8. The pixel randomization was removed during the reprocessing and the readout streaks were also removed for each observational data. The point sources are detected by `wavdetect` tool then point sources are removed for all ObsID. Spectra were extracted for the source region from the individual event files using the specextract script and spectral fitting was done with SHERPA package, assuming the simplest model consisting of the absorbed power-law. We have analyzed all the available *Chandra* data for the Western and Eastern hotspot of Pictor A. These include Chandra calibration observations as well as dedicated pointings. The Chandra data binned with a factor of 1 and 0.5 pixel for Western hotspot.

The Results

We have performed the Chandra image deconvolution analysis for the bright Western hotspot in Pictor A, resolving clearly its Mach disk structure (see Meisenheimer et al. 1989), as shown in Figure 1 for the ObsID 346. In the deconvolved images, we also confirmed (after a tentative finding by Hardcastle et al. 2016) a variability of the X-ray emission of the hotspot on the timescale of several years, as shown in Figure 2. The observed flux changes are unexpected, since the spatial extension of the terminal shock, illustrated as the projected (across the shock) surface brightness profile in Figure 3, is of the order of kpc; this would imply (through the light-crossing argument) the variability timescale of the order of thousands of years.

For the Eastern hotspot, characterized by a lower X-ray surface brightness and much worse Chandra coverage when compared with the Western hotspot, we performed a detailed X-ray spectral analysis of various regions, selected based on the observed correlation between the X-ray intensity and the polarized radio intensity, as shown in Figure 4; these include five bright compact X-ray spots, which may be unrelated foreground/background sources, and three diffuse regions. The results of the fitting (assuming the unabsorbed power-law model; combined fitting using the C-stat) are summarised below in the table. In general, the spectral analysis implies that the diffuse X-ray emission regions coinciding with the polarized radio filaments, are characterized by photon indices $\Gamma \sim 1.7 - 2.2$, while the majority of the point sources have $\Gamma \leq 1.2$.

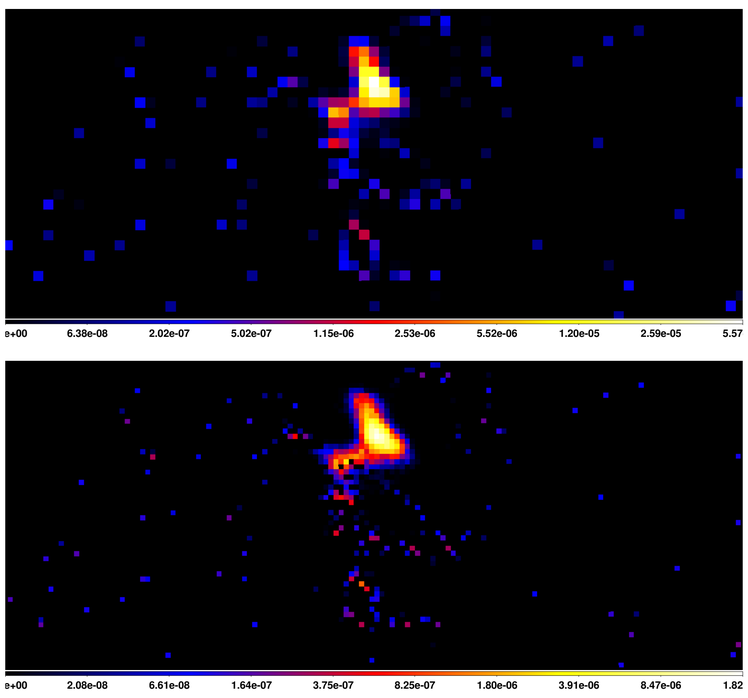

Figure 1: The deconvolved image of the Western hotspot (the average restored images for 100 iterations in the LRDA). Upper panel: 1 pix resolution, Lower panel: 0.5 pix resolution). ObsID 346

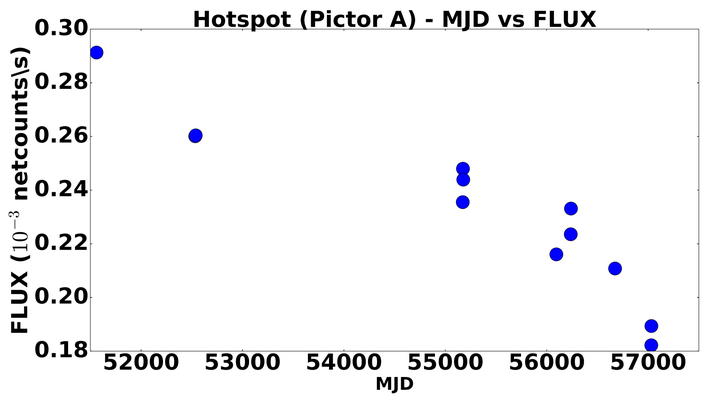

Figure 2: The flux (netcounts/s) in the energy of 0.5-7 keV for the W hotspot as a function of observing time.

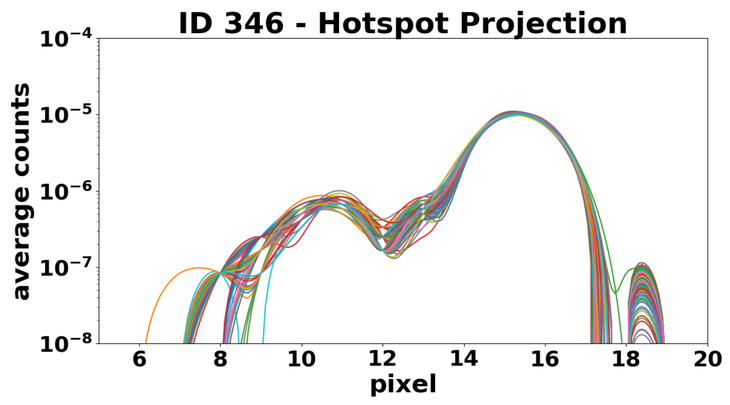

Figure 3: Projected (across the shock) surface brightness profile of the western hotspot (bin=1 px). ObsID 346

Figure 4: The polarized radio intensity contours 9from Perley et al. 1997) superimposed on the x-ray (0.5-7.0 keV) map of the Eastern hotspot region.

Regions	PhoIndex(Γ)
A	$1.70116^{+0.232}_{-0.214}$
B	$1.89136^{+0.555}_{-0.461}$
C	$2.16929^{+0.625}_{-0.534}$
P1	$2.26511^{+0.374}_{-0.341}$
P2	$2.15320^{+0.418}_{-0.389}$
P3	$0.42780^{+0.712}_{-0.743}$
P4	$1.13064^{+0.306}_{-0.297}$
P5	$1.02370^{+0.583}_{-0.568}$
background	$0.27227^{+0.026}_{-0.026}$

Conclusions & Future work

- The X-ray variability of the Western hotspot, observed on the timescale of years, implies an extreme substructre of the targeted relativistic shock.
- The various regions in the Eastern hotspot reveal various levels of the correlation between the X-ray intensity and the polarized radio intensity.
- The next step of the analysis will include a detailed point-to-point correlation analysis between the X-ray fluxes and radio (total and polarized) fluxes of the extended lobes in the system.

References

Hardcastle, M. J., Lenc, E., Birkinshaw, M., et al. 2016, MNRAS, 455, 3526
Meisenheimer, K., Roser, H.-J., et al. 1989, A&A, 219, 86
Perley, R. A., Roser, H.-J., & Meisenheimer, K. 1997, A&A, 328, 12

Acknowledgement

This work was supported by the Polish National Science Centre through the grant 2016/22/E/ST9/00061 and DSC grant 2019-N17/MNS/000046